Isotropic Streaming Effects in Thermal Lattices

Alain Hébert
DEN/DM2S/SERMA/LENR
CEA Saclay
91191 Gif-sur-Yvette Cedex, France
alain.hebert@cea.fr

Keywords: Lattice calculation, Leakage model, Diffusion coefficient

Abstract

This work was carried out with a view to improve the calculation of the diffusion coefficients in situations where the isotropic streaming effects cannot be neglected. The proposed approach is based on a generalization of the homogeneous B_n model currently used in current–generation thermal lattice codes. The ECCO isotropic streaming model, originally developed for fast lattice problems, is generatized and applied to thermal lattice problems. Numerical results are emphasizing typical situations of pressurised water reactor lattice calculations: assembly homogenization of a MOX–fuelled assembly surrounded by UOX assemblies and calculation of assembly–dependent diffusion coefficients.

1 INTRODUCTION

A leakage model is required in a lattice calculation performed with a *fundamental mode* approximation, i.e., when the elementary cell or assembly calculation is performed in 2D and/or is surrounded by reflection or translation boundary conditions. Any axial and/or radial leakage rate not taken into account by an explicit boundary condition must be represented by the leakage model. The leakage rate depends of the following factors:

- scattering anisotropy
- streaming effects caused by strong heterogeneities and/or low optical density regions in the lattice

Moreover the leakage model is used to obtain consistent values of the diffusion coefficients that can be used in a full core reactor calculation performed with the diffusion equation. Taking into account the streaming effects leads to a truly heterogeneous definition of the diffusion coefficient.

The streaming effect can be isotropic or anisotropic, depending if the leakage rate is identical or different for the three spatial dimensions. Isotropic streaming is mainly caused by heterogeneities of the lattice, such as poison pins or finite regions of small optical density. Anisotropic streaming is due to the fact that the lattice may not have the same properties along the axial dimension and over the radial plane of the lattice. Anisotropic streaming effects are worsen by the presence of leakage channels (a voided zone along the axial dimension) and of leakage planes (a voided zone along an infinite plane). The modelization of anisotropic streaming effect is mainly required for the processing of unit cells with gazeous coolant and of voided lattices.

The scattering anisotropy can be neglected in some fast reactor cases. It is therefore possible to use a non–consistent leakage model and to correct scattering anisotropy with a transport correction. For the case of an experimental facility similar to MASURCA where the leakage is important, it have

been shown that the effect of sacttering anisotropy cannot be neglected. This effect is of the order of $\sim$ 100 pcm, greater than the experimental uncertainty. Morever, the streaming effects can *never* be neglected.

In a pressurized water reactor (PWR), the effect of scattering anisotropy on the leakage is of prime importance, due to the presence of hydrogen in the moderator. Its effect on the leakage model is therefore *always* taken into account by using a consistent B_1 approximation. However, the streaming effects can often be neglected, except in some specific cases:

- in a loss of coolant accident (LOCA) –type calculation
- assembly homogenization of a MOX–fuelled assembly surrounded by UOX assemblies
- and for the calculation of pin–dependent diffusion coefficients, if some poison pins or empty channels are present.

In other cases, an homogeneous consistent B_1 calculation is sufficient, as proposed in [Kavenoky, 1968, Sanchez, 1987].

The first section describes the homoheneous B_n model, currently used to represent leakage rates in the APOLLO family of thermal lattice codes. The ECCO model is next presented as an alternative to better compute isotropic streaming effects caused by lattice heterogeneities [Grimstone, 1990]. We finally explain how we successfully adapted the ECCO model to the specific iterative strategy of a thermal lattice code.

2 THE B_n LEAKAGE CALCULATION

In a lattice calculation, we need to determine neutron fluxes, leakage and reaction rates of a unit cell or assembly *without* the knowledge of the exact operating conditions and materials surrounding it. However, we can always assume that the real neutron flux of the unit cell or assembly is under steady-state conditions (i.e., we know that $K_{\text{eff}} = 1$).

Without more information, the best that we can do in the lattice calculation is to assume that all the surrounding cells or assemblies are *identical* to the one being considered and to adjust the neutron leakage in each group g in such a way that $K_{\text{eff}} = 1$. We will adopt the following strategy:

1. The flux calculation inside the unit cell or assembly will be performed under *closed* conditions. An infinite domain or a finite domain closed with reflective (i.e., with an albedo set to 1) or periodic boundary conditions will be used. Note that this restriction is also required within the resonance self-shielding model and within the SPH equivalence technique [Hébert, 1993].

2. A leakage model will be introduced to enforce $K_{\text{eff}} = 1$ in the unit cell or assembly. This is done in most lattice codes by introducing a *fundamental mode* approximation. The principle is to represent the neutron flux as the product of a macroscopic distribution in space $\psi(\vec{r})$ with a homogeneous or periodic *fundamental* flux $\varphi(\vec{r}, E, \vec{\Omega})$. In any case, the flux factorization is written

$$\phi(\vec{r}, E, \vec{\Omega}) = \psi(\vec{r})\ \varphi(\vec{r}, E, \vec{\Omega}) \quad . \tag{1}$$

3. In the context of the fundamental mode approximation applied over a global reactor featuring a periodic lattice of unit cells or assemblies, the macroscopic distribution is assumed to be a property of the complete reactor and to be the solution of a Laplace equation:

$$\nabla^2\psi(\vec{r}) + B^2\,\psi(\vec{r}) = 0 \tag{2}$$

where the *buckling* B^2 is a real number that is used to adjust the curvature of $\psi(\vec{r})$ in such a way to obtain $K_{\text{eff}} = 1$. The buckling is positive or negative if the lattice is originally over-critical or sub-critical. The curvature thus obtained must be similar to what is observed for the real neutron flux in the complete reactor.

There exist homogeneous and heterogeneous varieties of the fundamental mode theory, depending on whether the fundamental flux $\varphi(\vec{r}, E, \vec{\Omega})$ is assumed to be homogeneous or periodic according to the lattice pitch. The heterogeneous fundamental mode approximation is used to take into account the streaming effects in the lattice.

Without any knowledge of the complete reactor geometry, we will use the following generic solution of Eq. (2):

$$\psi(\vec{r}) = \psi_0\; e^{i\vec{B}\cdot\vec{r}} \tag{3}$$

where the vector $\vec{B}$ is chosen in such a way that $B^2 = \vec{B}\cdot\vec{B}$. The neutron flux will therefore be factorized as

$$\phi(\vec{r}, E, \vec{\Omega}) = \varphi(\vec{r}, E, \vec{\Omega})\; e^{i\vec{B}\cdot\vec{r}} \tag{4}$$

where $\varphi(\vec{r}, E, \vec{\Omega})$ is a complex value.

The determination of the corresponding leakage rates in each energy group will be obtained through the *homogeneous* or *heterogeneous* B_1 *equations*. These equations are obtained after performing the factorization of Eq. (1) into the Boltzmann equation applied to a finite lattice of cells or assemblies.

3 THE HOMOGENEOUS FUNDAMENTAL MODE

This model assumes that the leakage rates can be computed in a unit cell (or assembly) completely homogenized in space. Note that the collision rates are nevertheless computed in the heterogeneous representation of the lattice.

The idea is therefore to to compute the curvature of the macroscopic flux distribution in the homogenized unit cell (or assembly). A flux–volume homogenization is generally performed. In this case, the factorization of Eq. (4) is rewritten as

$$\phi(\vec{r}, E, \vec{\Omega}) = \varphi(E, \vec{\Omega})\; e^{i\vec{B}\cdot\vec{r}} \tag{5}$$

where we note the non–dependence of $\varphi(E, \vec{\Omega})$ with the spatial coordinates. This value is complex.

3.1 The homogeneous B_1 equations

The next step consists to obtain the Boltzmann equation for the case of a finite and homogeneous geometry. The detail of the demonstration is given in reference [Hébert, 1997]. We obtain:

$$\begin{aligned} \vec{\Omega}\cdot\nabla\phi(\vec{r}, E, \vec{\Omega}) \;+\; & \Sigma(E)\;\phi(\vec{r}, E, \vec{\Omega}) \\ = \; & \int_{4\pi} d^2\Omega' \int_0^\infty dE'\; \Sigma_{\text{s}}(E \leftarrow E', \vec{\Omega} \leftarrow \vec{\Omega}')\;\phi(\vec{r}, E', \vec{\Omega}') \\ + \; & \frac{\chi(E)}{4\pi\; K_{\text{eff}}} \int_0^\infty dE'\; \nu(E')\;\Sigma_{\text{f}}(E')\;\phi(\vec{r}, E') \end{aligned} \tag{6}$$

where

$\Sigma_{\rm s}(E \leftarrow E', \vec{\Omega} \leftarrow \vec{\Omega}') =$ macroscopic differential scattering cross section taking into account diffusion *and* (n,xn) reactions.

$\chi(E) =$ fission spectrum (normalized to 1)

$\Sigma(E) =$ macroscopic total cross section

$\Sigma_{\rm f}(E) =$ macroscopic fission cross section

$\nu(E) =$ average number of secondary neutrons per fission (taking into account delayed neutrons)

$\phi(\vec{r}, E, \vec{\Omega}) =$ angular flux

$\phi(\vec{r}, E) =$ scalar flux.

The corresponding homogeneous B_1 equations are obtained by substituting the factorization (5) into Eq. (6). We obtain:

$$\begin{aligned} \left[\Sigma(E) + i\vec{B}\cdot\vec{\Omega}\right]\varphi(E,\vec{\Omega}) &= \int_{4\pi} d^2\Omega' \int_0^\infty dE'\, \Sigma_{\rm s}(E \leftarrow E', \vec{\Omega} \leftarrow \vec{\Omega}')\, \varphi(E', \vec{\Omega}') \\ &+ \frac{\chi(E)}{4\pi\, K_{\rm eff}} \int_0^\infty dE'\, \nu(E')\, \Sigma_{\rm f}(E')\, \varphi(E') \end{aligned} \tag{7}$$

where the scalar fundamental flux is given in terms of the angular fundamental flux using

$$\varphi(E) = \int_{4\pi} d^2\Omega\, \varphi(E,\vec{\Omega}) \quad . \tag{8}$$

We next expand the differential scattering term using zero and first order Legendre polynomials. This expansion is the equivalent of assuming a linearly anisotropic collision in the laboratory frame. We obtain

$$\Sigma_{\rm s}(E \leftarrow E', \vec{\Omega} \leftarrow \vec{\Omega}') = \frac{1}{2\pi}\Sigma_{\rm s}(E \leftarrow E', \mu) = \sum_{\ell=0}^{1} \frac{2\ell+1}{4\pi}\, \Sigma_{{\rm s},\ell}(E \leftarrow E')\, P_\ell(\mu) \tag{9}$$

where $\mu = \vec{\Omega}\cdot\vec{\Omega}'$, $P_0(\mu) = 1$ and $P_1(\mu) = \mu$.
It is useful to remember that the ℓ-th order Legendre coefficient of the differential scattering cross section is given as

$$\Sigma_{{\rm s},\ell}(E \leftarrow E') = \int_{-1}^{1} d\mu\, \Sigma_{\rm s}(E \leftarrow E', \mu)\, P_\ell(\mu) \;\; ; \;\; \ell \geq 0 \tag{10}$$

Substituting Eq. (9) into Eq. (7), we get

$$\begin{aligned} \left[\Sigma(E) + i\vec{B}\cdot\vec{\Omega}\right]\varphi(E,\vec{\Omega}) &= \int_0^\infty dE' \left\{\frac{1}{4\pi}\Sigma_{\rm s0}(E \leftarrow E')\, \varphi(E') \right. \\ &+ \left. \frac{3}{4\pi}\Sigma_{\rm s1}(E \leftarrow E')\, \vec{\mathcal{J}}(E')\cdot\vec{\Omega}\right\} \\ &+ \frac{\chi(E)}{4\pi\, K_{\rm eff}} \int_0^\infty dE'\, \nu(E')\, \Sigma_{\rm f}(E')\, \varphi(E') \end{aligned} \tag{11}$$

where the *fundamental current* is given in terms of the angular fundamental flux using

$$\vec{\mathcal{J}}(E) = \int_{4\pi} d^2\Omega \; \vec{\Omega} \; \varphi(E, \vec{\Omega}) \quad . \tag{12}$$

Eq. (11) is weighted and integrated over $\vec{\Omega}$ as required by the B_1 model:

1. A simple integration, without weighting, leads to the first B_1 equation (a conservation relation). Some terms have been removed due to parity properties:

$$\begin{aligned} \Sigma(E) \; \varphi(E) + iB \; \mathcal{J}(E) &= \int_0^\infty dE' \; \Sigma_{\mathrm{s0}}(E \leftarrow E') \; \varphi(E') \\ &+ \frac{\chi(E)}{K_{\mathrm{eff}}} \int_0^\infty dE' \; \nu(E') \; \Sigma_{\mathrm{f}}(E') \; \varphi(E') \end{aligned} \tag{13}$$

   where the dependency against the direction of vector $\vec{B}$ was removed by defining

$$\mathcal{J}(E) = \frac{1}{B} \; \left[\vec{B} \cdot \vec{\mathcal{J}}(E) \right] \quad . \tag{14}$$

2. The weight factor

$$\omega(\vec{\Omega}) = \frac{1}{\Sigma(E) + i\vec{B} \cdot \vec{\Omega}}$$

   is next used to multiply each member of Eq. (11) before its integration:

$$\begin{aligned} \varphi(E) &= \int_0^\infty dE' \left\{ \frac{1}{4\pi} \Sigma_{\mathrm{s0}}(E \leftarrow E') \; \varphi(E') \int_{4\pi} d^2\Omega \; \frac{\Sigma(E) - i\vec{B} \cdot \vec{\Omega}}{\Sigma(E)^2 + (\vec{B} \cdot \vec{\Omega})^2} \right. \\ &+ \left. \frac{3}{4\pi} \Sigma_{\mathrm{s1}}(E \leftarrow E') \; \vec{\mathcal{J}}(E') \cdot \int_{4\pi} d^2\Omega \; \frac{\vec{\Omega} \; \Sigma(E) - i \; (\vec{\Omega} \otimes \vec{\Omega}) \cdot \vec{B}}{\Sigma(E)^2 + (\vec{B} \cdot \vec{\Omega})^2} \right\} \\ &+ \frac{\chi(E)}{4\pi \; K_{\mathrm{eff}}} \int_0^\infty dE' \; \nu(E') \; \Sigma_{\mathrm{f}}(E') \; \varphi(E') \int_{4\pi} d^2\Omega \; \frac{\Sigma(E) - i\vec{B} \cdot \vec{\Omega}}{\Sigma(E)^2 + (\vec{B} \cdot \vec{\Omega})^2} \; . \end{aligned}$$

   After some simplification relating to parity properties, we obtain

$$\begin{aligned} \varphi(E) &= \alpha \left[B, \Sigma(E) \right] \left\{ \int_0^\infty dE' \; \Sigma_{\mathrm{s0}}(E \leftarrow E') \; \varphi(E') \right. \\ &+ \left. \frac{\chi(E)}{K_{\mathrm{eff}}} \int_0^\infty dE' \; \nu(E') \; \Sigma_{\mathrm{f}}(E') \; \varphi(E') \right\} \\ &- 3i \; \beta \left[B, \Sigma(E) \right] \; B \int_0^\infty dE' \; \Sigma_{\mathrm{s1}}(E \leftarrow E') \; \mathcal{J}(E') \end{aligned} \tag{15}$$

   where we used the following identities:

$$\frac{1}{4\pi} \int_{4\pi} d^2\Omega \; \frac{\Sigma^2}{\Sigma^2 + (\vec{B} \cdot \vec{\Omega})^2} = \alpha(B, \Sigma) \; \Sigma \tag{16}$$

and

$$\frac{1}{4\pi}\int_{4\pi} d^2\Omega\ \frac{(\vec{\Omega}\otimes\vec{\Omega})\cdot\vec{B}}{\Sigma^2+(\vec{B}\cdot\vec{\Omega})^2} = \beta(B,\Sigma)\ \vec{B} \quad . \tag{17}$$

The functions $\alpha(B,\Sigma)$ and $\beta(B,\Sigma)$ are defined as

$$\alpha(B,\Sigma) = \begin{cases} \frac{1}{B}\ \arctan\frac{B}{\Sigma} & \text{if } B^2 > 0; \\ \frac{1}{\Sigma} - \frac{B^2}{3\Sigma^3} + \frac{B^4}{5\Sigma^5} - \frac{B^6}{7\Sigma^7} + \dots & \text{if } B^2 \simeq 0; \\ \frac{1}{2\Im(B)}\ \ln\frac{\Sigma+\Im(B)}{\Sigma-\Im(B)} & \text{if } B^2 < 0. \end{cases} \tag{18}$$

where $\Im(B)$ is the imaginary component of B and

$$\beta(B,\Sigma) = \frac{1}{B^2}\ [1-\alpha(B,\Sigma)\ \Sigma] \quad . \tag{19}$$

The second B_1 equation is finally obtained by substituting Eq. (13) into Eq. (15) and by reordering the terms:

$$\frac{i\mathcal{J}(E)}{B} = \frac{1}{\Sigma(E)\ \gamma\left[B,\Sigma(E)\right]}\left\{\frac{1}{3}\ \varphi(E) + \int_0^\infty dE'\ \Sigma_{\text{s1}}(E\leftarrow E')\ \frac{i\mathcal{J}(E')}{B}\right\} \tag{20}$$

where

$$\gamma(B,\Sigma) = \frac{1}{3\Sigma}\ \frac{\alpha(B,\Sigma)}{\beta(B,\Sigma)} \simeq 1 + \frac{4}{15}\left(\frac{B}{\Sigma}\right)^2 - \frac{12}{175}\left(\frac{B}{\Sigma}\right)^4 + \frac{92}{2625}\left(\frac{B}{\Sigma}\right)^6 + \dots \quad . \tag{21}$$

Eqs. (13) and (20) form the coupled set of the two B_1 equations. We did assume linearly anisotropic scattering in the laboratory frame, but no $\vec{\Omega}$-expansion of the angular fundamental flux was required. In homogeneous cases, we also observe that the fundamental flux $\varphi(E)$ is always real and that the fundamental current $\mathcal{J}(E)$ is whether imaginary or real, depending if the homogeneous medium is super- or sub-critical. However, the quantity $i\mathcal{J}(E)/B$ is always real and remains finite when the buckling approaches zero.

This system can be solved using a multigroup discretization, taking care to use a sufficiently large number of energy groups to ensure that

$$\langle\gamma(B,\Sigma)\rangle_g \simeq \gamma\left[B,\langle\Sigma\rangle_g\right] \quad . \tag{22}$$

These equations are also used to find the *critical buckling*, i.e., the value of B^2 that will lead to an effective multiplication factor K_{eff} equal to one.

Note that the *inconsistent* B_1 form of the homogeneous leakage model is obtained by assuming $\Sigma_{\text{s1}}(E\leftarrow E') = 0$ in Eq. (20). A transport correction can be applied to the macroscopic total cross section $\Sigma(E)$ in order to improve the accuracy of the model. This inconsistent form of the leakage model should never be used in presence of hydrogen–based moderators.

3.2 The leakage rates.

The *leakage coefficient* is defined as

$$d(B,E) = \frac{1}{B}\,\frac{i\mathcal{J}(E)}{\varphi(E)} \tag{23}$$

and used as a change of variable relation to transform Eqs. (13) and (20). A new set of B_1 equations are then obtained:

$$\begin{aligned}\left[\Sigma(E) + d(B,E)\;B^2\right]\varphi(E) \;&=\; \int_0^\infty dE'\;\Sigma_{\rm s0}(E \leftarrow E')\;\varphi(E') \\ &+\; \frac{\chi(E)}{K_{\rm eff}}\int_0^\infty dE'\;\nu(E')\,\Sigma_{\rm f}(E')\;\varphi(E')\end{aligned} \tag{24}$$

and

$$d(B,E) = \frac{1}{3\gamma\,[B,\Sigma(E)]\;\Sigma(E)}\left\{1 + 3\int_0^\infty dE'\;\Sigma_{\rm s1}(E \leftarrow E')\;d(B,E')\;\frac{\varphi(E')}{\varphi(E)}\right\} \quad . \tag{25}$$

We observe that Eq. (24) can be easily condensed over any energy group structure if we use the following group-averaged values:

$$\varphi_g = \int_{E_g}^{E_{g-1}} dE\;\varphi(E) \quad , \tag{26}$$

$$d_g = \frac{1}{\varphi_g}\int_{E_g}^{E_{g-1}} dE\;d(B,E)\;\varphi(E) \tag{27}$$

and

$$\Sigma_g = \frac{1}{\varphi_g}\int_{E_g}^{E_{g-1}} dE\;\Sigma(E)\;\varphi(E) \quad . \tag{28}$$

The group-dependent leakage rate L_g appears naturally as

$$L_g = d_g\;B^2\;\bar{\varphi}_g \quad . \tag{29}$$

The principle behind an homogeneous leakage model is to modify the heterogeneous flux equation with an additional term defined in such a way to force the homogeneous leakage rate of Eq. (29). With this correction, the volume average of the heterogeneous flux $\bar{\phi}_g$ is equal to the fundamental flux φ_g of the homogeneous B_1 model. This technique can be applied to all deterministic solution techniques of the Boltzmann equation. As an example, we are presenting its application to the collision probability technique.

3.3 Application to the collision probability technique

The collision probability technique is based on a multigroup discretization and allow the calculation of the neutron flux into the heterogeneous regions of the cell or of the assembly. The flux is given by the relation

$$\phi_{i,g} = \sum_j Q_{j,g}\ \tilde{p}_{ij,g} \tag{30}$$

where

$\phi_{i,g} =$ neutron flux in region g and region i

$Q_{j,g} =$ scattering and fission neutron source

$\Sigma_{i,g} =$ macroscopic total cross section

$\tilde{p}_{ij,g} =$ reduced collision probability. $\tilde{p}_{ij,g}\Sigma_{j,g}$ is the probability for a neutron born uniformally and isotropically in region i to undergo its first collision in region j.

In order to reach a faster convergence, the within-group scattering term is removed from the source term:

$$\phi_{i,g} - \sum_j p_{ij,g}\ \Sigma_{\mathrm{s0},j,g\leftarrow g}\ \phi_{j,g} = \sum_j Q^*_{j,g}\ \tilde{p}_{ij,g} \tag{31}$$

where the source term $Q^*_{i,g}$ does not include the contributions from the within–group scattering rates in group g. The modified source term is written as

$$Q^*_{i,g} = \sum_{h\neq g} \Sigma_{\mathrm{s0},i,g\leftarrow h}\ \phi_{i,h}\ +\ \frac{1}{K_{\mathrm{eff}}} Q^{\mathrm{fiss}}_{i,g} \tag{32}$$

where

$\Sigma_{\mathrm{s0},i,g\leftarrow h} =$ macroscopic transfer cross section for the scattering reaction

$Q^{\mathrm{fiss}}_{i,g} =$ source of secondary neutrons from fission.

Eq. (31) can be written in matrix form as

$$\vec{\phi}_g = \mathbf{W}_g \vec{Q}^*_g \tag{33}$$

where $\vec{\phi}_g = \{\phi_{i,g}\ ;\ \forall i\}$ and $\vec{Q}^*_g = \{Q^*_{i,g}\ ;\ \forall i\}$.

$\mathbf{W}_g$ is a scattering reduced collision probability matrix, defined as

$$\mathbf{W}_g = [\mathbf{I} - \mathbf{p}_g\ \mathbf{\Sigma}_{\mathrm{s0},g\leftarrow g}]^{-1}\mathbf{p}_g \tag{34}$$

where $\mathbf{I}$ is the identity matrix, $\mathbf{p}_g = \{p_{ij,g}\ ;\ \forall i \text{ et } j\}$ and $\mathbf{\Sigma}_{\mathrm{s0},g\leftarrow g} = \mathrm{diag}\{\Sigma_{\mathrm{s0},i,g\leftarrow g}\ ;\ \forall i\}$.

The leakage rate obtained from the fundamental mode model can be included in Eq. (34) by substracting $d_g(B)\ B^2$ from the within-group scattering cross sections. Eq. (33) is then replaced by

$$\vec{\phi}_g = \mathbf{W}_g \left[\vec{Q}^*_g - d_g(B)\ B^2\ \vec{\phi}_g\right] \tag{35}$$

where transport-corrected total cross sections are used to compute the $\mathbf{W}_g$ matrix. This is the so called *DIFFON method* used in the APOLLO-family of thermal lattice codes.

Another possibility is to increase the transport-corrected macroscopic total cross sections of the subregions by a component equal to $d_g(B)\ B^2$. This solution would not be cost-effective as it would impose recomputing the CPs during the critical buckling search.

3.4 The diffusion coefficient.

The diffusion coefficient is the proportionality factor $D(\vec{r}, E)$ introduced to relate the net current $\vec{J}(\vec{r}, E)$ with the gradient of the flux:

$$\vec{J}(\vec{r}, E) = -D(\vec{r}, E)\ \nabla\phi(\vec{r}, E) \quad . \tag{36}$$

The diffusion coefficient can be calculated for a fundamental mode situation, even in homogenized lattice cases. In this case, we simply use factorizations compatible with Eq. (4):

$$\phi(\vec{r}, E) = \varphi(E)\ e^{i\vec{B}\cdot\vec{r}} \tag{37}$$

and

$$\vec{J}(\vec{r}, E) = \vec{\mathcal{J}}(E)\ e^{i\vec{B}\cdot\vec{r}} \quad . \tag{38}$$

Taking the gradient of Eq. (37), we obtain

$$\nabla\phi(\vec{r}, E) = i\vec{B}\ \varphi(E)\ e^{i\vec{B}\cdot\vec{r}} \quad . \tag{39}$$

Substitution of Eqs. (38) and (39) into Eq. (36) and use of Eq. (14) leads to the following definition of the diffusion coefficient:

$$D(\vec{r}, E) = d(B, E) = \frac{1}{B}\ \frac{i\mathcal{J}(E)}{\varphi(E)} \quad . \tag{40}$$

We have demonstrated that the diffusion coefficient, as obtained from the B_1 equations, is uniform in the lattice and equal to the leakage coefficient. Multigroup diffusion coefficients (including two-group values) can be consistently obtained from Eq. (27). These values will be used in the few-group reactor calculation based on the diffusion theory.

4 THE HETEROGENEOUS FUNDAMENTAL MODE

An heuristic approach, based on a B_1 consistent model, was originally developed in the ECCO fast lattice code[Grimstone, 1990] in an attempt to combine features of the homogeneous B_n model with heterogeous effects of a collision probability calculation. The ECCO model is recommended to represent the effects of scattering anisotropy on the leakage rates and the isotropic streaming effects due to low optical density and neutron feeding zones in the lattice. However, the ECCO model is not recommended to represent the anisotropic streaming effects induced by coolant voiding along infinite planes.

We propose to generalize the ECCO model to other types of flux solution algorithms and to use it in the context of thermal lattice calculations. The ECCO approach assumes the isotropy of the streaming effects. It consists of merging Eqs. (13) and (20) (B_1 equations) with the flux Eq. (30) of the collision probability method:

$$\varphi_{i,g} = \sum_j \left(Q_{j,g} - B^2\ \frac{i\mathcal{J}_{j,g}}{B}\right)\ \tilde{p}_{ij,g} \tag{41}$$

$$\frac{i\mathcal{J}_{i,g}}{B} = \frac{1}{\gamma(B, \bar{\Sigma}_g)} \sum_j \left(\frac{1}{3}\ \varphi_{j,g} + \sum_h \Sigma_{\mathrm{s1},j,g\leftarrow h}\ \frac{i\mathcal{J}_{j,h}}{B}\right) \tilde{p}_{ij,g} \tag{42}$$

where $\bar{\Sigma}_g$ is the average in group g of the total macroscopic cross section, weighted with the flux $\varphi_{i,g}$ and the volumes.

This approach leads to an heterogeneous leakage coefficient (or diffusion coefficient) given by

$$d_{i,g} = \frac{1}{B}\,\frac{i\mathcal{J}_{i,g}}{\varphi_{i,g}} \quad . \tag{43}$$

In order to reach a faster convergence, the within-group scattering term is removed from the source term:

$$\begin{aligned}
\varphi_{i,g} - \sum_j p_{ij,g}\,\Sigma_{\mathrm{s0},j,g\leftarrow g}\,\varphi_{j,g} &= \sum_j \left(Q^*_{j,g} - B^2\,\frac{i\mathcal{J}_{j,g}}{B}\right)\,\tilde{p}_{ij,g} \\
\frac{i\mathcal{J}_{i,g}}{B} - \sum_j p_{ij,g}\,\Sigma_{\mathrm{s1},j,g\leftarrow g}\,\frac{i\mathcal{J}_{j,g}}{B} &= \frac{1}{\gamma(B,\bar{\Sigma}_g)}\sum_j \left[\frac{1}{3}\,\varphi_{j,g} + \sum_{h\neq g}\Sigma_{\mathrm{s1},j,g\leftarrow h}\,\frac{i\mathcal{J}_{j,h}}{B}\right. \\
&\quad \left. + \Big(1-\gamma(B,\bar{\Sigma}_g)\Big)\,\Sigma_{\mathrm{s1},j,g\leftarrow g}\,\frac{i\mathcal{J}_{j,g}}{B}\right]\tilde{p}_{ij,g} \quad .
\end{aligned} \tag{44}$$

These equations are next rewritten in matrix form as

$$\vec{\varphi}_g = \mathbf{W}_g\left(\vec{Q}^*_g - B^2\,\frac{i\vec{\mathcal{J}}_{j,g}}{B}\right) \tag{45}$$

$$\frac{i\vec{\mathcal{J}}_g}{B} = \frac{1}{\gamma(B,\bar{\Sigma}_g)}\,\mathbf{X}_g\left[\frac{1}{3}\,\vec{\varphi}_g + \sum_{h\neq g}\mathbf{\Sigma}_{\mathrm{s1},g\leftarrow h}\,\frac{i\vec{\mathcal{J}}_h}{B} + \Big(1-\gamma(B,\bar{\Sigma}_g)\Big)\,\mathbf{\Sigma}_{\mathrm{s1},g\leftarrow g}\,\frac{i\vec{\mathcal{J}}_g}{B}\right] \tag{46}$$

where $\mathbf{\Sigma}_{\mathrm{s1},g\leftarrow h} = \mathrm{diag}\{\Sigma_{\mathrm{s1},i,g\leftarrow h}\,;\,\forall i\}$ and where

$$\mathbf{X}_g = [\mathbf{I} - \mathbf{p}_g\,\mathbf{\Sigma}_{\mathrm{s1},g\leftarrow g}]^{-1}\mathbf{p}_g \quad . \tag{47}$$

It is worth noting that Eq. (42) of the ECCO model uses macroscopic cross sections which are *not* transport–corrected. The linear system made of Eqs. (45) and (46) is generally solved iteratively. In case of slow convergence, as it is often the case with thermal lattice problems, it is possible to use a rebalancing strategy based on the homogeneous B_1 equation.

This ECCO model is equivalent to the TIBÈRE model with the assumption of the isotropy of the fundamental current (i.e., when the 3 components of the fundamental current (12) are equal). TIBÈRE is a fundamental mode model, featuring heteroneneous and anisotropic leakage effects, originally developed by P. Benoist [Benoist, 1994].

The integro-differential form of the ECCO model can be written:

$$\vec{\Omega}\cdot\nabla\varphi(\vec{r},E,\vec{\Omega}) + \Sigma(\vec{r},E)\,\varphi(\vec{r},E,\vec{\Omega}) = \frac{1}{4\pi}\,\left[Q(\vec{r},E) - iB\mathcal{J}(\vec{r},E)\right] \tag{48}$$

$$\begin{aligned}
\vec{\Omega}\cdot\nabla\frac{i\mathcal{J}(\vec{r},E,\vec{\Omega})}{B} + \Sigma(\vec{r},E)\,\frac{i\mathcal{J}(\vec{r},E,\vec{\Omega})}{B} &= \frac{1}{4\pi\,\gamma\left[B,\bar{\Sigma}_0(E)\right]}\left[\frac{1}{3}\,\varphi(\vec{r},E)\right. \\
&\quad \left. + \int_0^\infty dE'\,\Sigma_{\mathrm{s1}}(\vec{r},E\leftarrow E')\,\frac{i\mathcal{J}(\vec{r},E')}{B}\right] \quad .
\end{aligned} \tag{49}$$

The ECCO model is probably the most accurate leakage model which can be combined with the integro-differential form of the Boltzmann equation. It is therefore compatible with all the available deterministic approaches, including the discrete ordinate and the characteristics methods. The cost overhead is small, enabling its use in production calculations such as burnup–dependent and feedback–type PWR assembly calculations. The ECCO model is also compatible with the interface current method and the related current–iterative algorithm used in the APOLLO–type calculation schemes.

4.1 Homogenization and condensation of lattice cross sections

The P_1 consistent form of Eqs. (48) and (49) can be written for a partially homogenized geometry and condensed energy mesh. Using a set of homogenized volumes $\{V_i,\ \forall\, i\}$ and macro groups $\{E_g,\ \forall\, g\}$, the following averaged values are first set:

$$\varphi_{i,g} = \frac{1}{\mu_{i,g}\ V_i} \int_{V_i} d^3r \int_{E_g}^{E_{g-1}} dE\ \varphi(\vec{r},E)\ \ , \tag{50}$$

$$\frac{i\mathcal{J}_{i,g}}{B} = \frac{1}{\mu_{i,g}\ V_i} \int_{V_i} d^3r \int_{E_g}^{E_{g-1}} dE\ \frac{i\mathcal{J}(\vec{r},E)}{B}\ \ , \tag{51}$$

$$\Sigma_{0,i,g} = \frac{\mu_{i,g}}{V_i\ \varphi_{i,g}} \int_{V_i} d^3r \int_{E_g}^{E_{g-1}} dE\ \Sigma(\vec{r},E)\ \varphi(\vec{r},E)\ \ , \tag{52}$$

$$\Sigma_{1,i,g} = \frac{\mu_{i,g}}{V_i \frac{i\mathcal{J}_{i,g}}{B}} \int_{V_i} d^3r \int_{E_g}^{E_{g-1}} dE\ \Sigma(\vec{r},E)\ \frac{i\mathcal{J}(\vec{r},E)}{B}\ \ , \tag{53}$$

$$\Sigma_{\mathrm{s0},i,g\leftarrow h} = \frac{\mu_{i,h}}{V_i\ \varphi_{i,h}} \int_{V_i} d^3r \int_{E_g}^{E_{g-1}} dE \int_{E_h}^{E_{h-1}} dE'\ \Sigma_{\mathrm{s0}}(\vec{r},E\leftarrow E')\ \varphi(\vec{r},E')\ \ , \tag{54}$$

and

$$\Sigma_{\mathrm{s1},i,g\leftarrow h} = \frac{\mu_{i,h}}{V_i \frac{i\mathcal{J}_{i,h}}{B}} \int_{V_i} d^3r \int_{E_g}^{E_{g-1}} dE \int_{E_h}^{E_{h-1}} dE'\ \Sigma_{\mathrm{s1}}(\vec{r},E\leftarrow E')\ \frac{i\mathcal{J}(\vec{r},E')}{B} \tag{55}$$

where $\mu_{i,g}$ is the SPH equivalence factor in region i and macrogroup g. These factors are computed using an equivalence procedure so as to to preserve the reaction rates over the homogenized and condensed mesh [Hébert, 1993]. We have used the same equivalence factor for the flux– and current–weighted cross sections, but this choice could be revised in the future.

We see that the linearly anisotropic component of the scattering cross section must be homogenized and condensed using the fundamental current. Moreover, we obtain two values for the total cross section, the first weighted with the fondamental flux and the second weighted with the fundamental current. These values, represented as $\Sigma_{0,i,g}$ and $\Sigma_{1,i,g}$, must respectively be used in the homogenized/condensed form of Eqs. (48) and (49).

If the full core calculation is performed using diffusion theory, consistency will be preserved by using the following definition for the heterogeneous diffusion coefficients:

$$D_{i,g} = \frac{\mu_{i,g}}{B}\ \frac{i\mathcal{J}_{i,g}}{\varphi_{i,g}}\ \ . \tag{56}$$

The diffusion equation can therefore be written as

$$-\nabla \cdot D_g(\vec{r})\nabla\phi_g(\vec{r}) + \Sigma_{0,g}(\vec{r})\ \phi_g(\vec{r}) = \sum_{h=1}^{G} \Sigma_{\mathrm{s}0,g\leftarrow h}\ \phi_h(\vec{r}) + \frac{1}{K_{\mathrm{eff}}} Q_g^{\mathrm{fiss}}(\vec{r}) \tag{57}$$

If the full core calculation is performed using the P_1 or SP_1 (for *Simplified* P_1) theory, we will use the cross section definitions (52) to (55). The P_1 or SP_1 can be written:

$$\nabla \cdot \vec{J}_g(\vec{r}) + \Sigma_{0,g}(\vec{r})\ \phi_g(\vec{r}) = \sum_{h=1}^{G} \Sigma_{\mathrm{s}0,g\leftarrow h}\ \phi_h(\vec{r}) + \frac{1}{K_{\mathrm{eff}}} Q_g^{\mathrm{fiss}}(\vec{r}) \tag{58}$$

$$\nabla\phi_g(\vec{r}) + 3\Sigma_{1,g}(\vec{r})\ \vec{J}_g(\vec{r}) = 3\sum_{h=1}^{G} \Sigma_{\mathrm{s}1,g\leftarrow h}\ \vec{J}_h(\vec{r}) \quad . \tag{59}$$

Care have been taken to use the total cross section $\Sigma_{0,g}$ in Eq. (58) and the total cross section $\Sigma_{1,g}$ in Eq. (59). This allow to recover the correct value of the diffusion coefficient in the limit where this model is applied to an homogeneous mixture. This value is given as

$$D_g = \frac{1}{3\Sigma_{1,g}} \left\{ 1 + 3\sum_{h} \Sigma_{\mathrm{s}1,g\leftarrow h}\ D_h\ \frac{\phi_h}{\phi_g} \right\} \tag{60}$$

which show the consistency of the cross section weighting used in Eqs. (58) and (59).

4.2 Homogenization consistent with the homogeneous B_n equations

The homogenization relations used in the preceding section are not fully compatible with the homogeneous B_n equations (13) and (20). Such an homogeneous calculation is nevertheless useful in the rebalancing algorithm of the power method or in the fixed point algorithm for converging on the critical buckling. The non consistency comes from the presence of the term $\gamma(B, \bar{\Sigma}_g)$ in Eq. (42) which is function of a flux–weighted total cross section. The consistency is recovered using a technique presented in reference [Petrovic, 1996].

The technique consists to add a corrective term to Eq. (49), leading to

$$\begin{aligned} \vec{\Omega}\cdot\nabla\frac{i\mathcal{J}(\vec{r},E,\vec{\Omega})}{B} \quad &+ \quad \Sigma(\vec{r},E)\ \frac{i\mathcal{J}(\vec{r},E,\vec{\Omega})}{B} = \frac{1}{4\pi\ \gamma\left[B,\bar{\Sigma}_0(E)\right]}\Big[\frac{1}{3}\ \varphi(\vec{r},E) \\ &+ \quad \int_0^{\infty} dE'\ \Sigma_{\mathrm{s}1}(\vec{r},E\leftarrow E')\ \frac{i\mathcal{J}(\vec{r},E')}{B} + \Delta(\vec{r},E)\frac{i\mathcal{J}(\vec{r},E)}{B}\Big] \end{aligned} \tag{61}$$

with

$$\Delta(\vec{r},E) = \Big(1-\gamma\left[B,\bar{\Sigma}_0(E)\right]\Big)\Big(\bar{\Sigma}_0(E) - \Sigma(\vec{r},E)\Big) \tag{62}$$

where $\bar{\Sigma}_0(E)$ is the average of the total cross section, weighted by the fundamental flux and volume. We note that this corrective term approaches zero if

- the lattice is homogeneous, or if
- the term $\gamma(B, \bar{\Sigma}_g)$ approaches 1.

Eq. (61) can be integrated in space and solid angles, leading to an homogenized equation compatible with the second B_1 Eq. (20):

$$\left\langle \frac{i\mathcal{J}(E)}{B} \right\rangle = \frac{1}{\bar{\Sigma}_0(E)\,\gamma\left[B,\bar{\Sigma}_0(E)\right]} \Big[\frac{1}{3}\,\langle\varphi(E)\rangle \;+\; \int_0^\infty dE'\,\bar{\Sigma}_{\mathrm{s1}}(E\leftarrow E')\,\left\langle \frac{i\mathcal{J}(E')}{B} \right\rangle + \left(\bar{\Sigma}_0(E)-\bar{\Sigma}_1(E)\right)\left\langle \frac{i\mathcal{J}(E)}{B} \right\rangle \Big] \tag{63}$$

where $\bar{\Sigma}_1(E)$ is the average of the total cross section, weighted with the fundamental current and volumes.

We note that the second B_1 Eq. (20) must be modified by a correcting term $\left(\bar{\Sigma}_0(E)-\bar{\Sigma}_1(E)\right)\frac{i\mathcal{J}(E)}{B}$ in cases it origin from the homogenization of an heterogeneous equation.

With the method of collision probabilities, Eq. (46) is modified as

$$\frac{i\vec{\mathcal{J}}_g}{B} = \frac{1}{\gamma(B,\bar{\Sigma}_{0,g})}\,\mathbf{X}_g \left(\frac{1}{3}\,\vec{\varphi}_g + \sum_{h\neq g} \mathbf{\Sigma}_{\mathrm{s1},g\leftarrow h}\,\frac{i\vec{\mathcal{J}}_h}{B} + \left(1-\gamma(B,\bar{\Sigma}_{0,g})\right)\mathbf{\Sigma}_{\mathrm{s1},g\leftarrow g}\,\frac{i\vec{\mathcal{J}}_g}{B} + \mathbf{\Delta}_g\frac{i\vec{\mathcal{J}}_g}{B} \right) \tag{64}$$

where $\mathbf{\Delta}_g = \mathrm{diag}\,\{\Delta_{i,g};\ \forall i\}$ with $\Delta_{i,g}$ equal to the value of $\Delta(\vec{r},E)$ in region i and group g.

5 NUMERICAL RESULTS

We studied a 2×2 colorset made of one mixed–oxyde (MOX) assembly and three uranium oxyde (UOX) assemblies. An eight–of–square symmetry representation was used, as shown in Fig. 1. The interface current method is used for both self-shielding and flux calculation. The cross sections of the MOX assembly are completely homogenized and condensed in two energy groups. Three approaches have been studied:

I An infinite lattice of MOX assemblies, without UOX environment, is solved with the homogeneous leakage model of Section 3.

II A colorset of MOX and UOX assemblies is solved with the homogeneous leakage model of Section 3. The MOX assembly is next homogenized with the application of SPH factors.

III A colorset of MOX and UOX assemblies is solved with the heterogeneous leakage model of Section 4. The MOX assembly is next homogenized with the application of SPH factors.

The representation of an UOX environment for a MOX assembly calculation is required in order to recover the correct flux spectrum on the MOX assembly boundary. For a MOX assembly computed without environment, the error on the Pu239 concentration can reach 30% in the periphery of the assembly. A non–depleting nominal UOX assembly is used in the environment. We choose a 3.25%–enriched UO_2 fuel burn to 24 GWday/tonne.

Table 1 shows the values of diffusion coefficients, transport corrected total cross sections and SPH factors obtained with the three approaches. The following conclusions can be stated from the analysis of the numerical results:

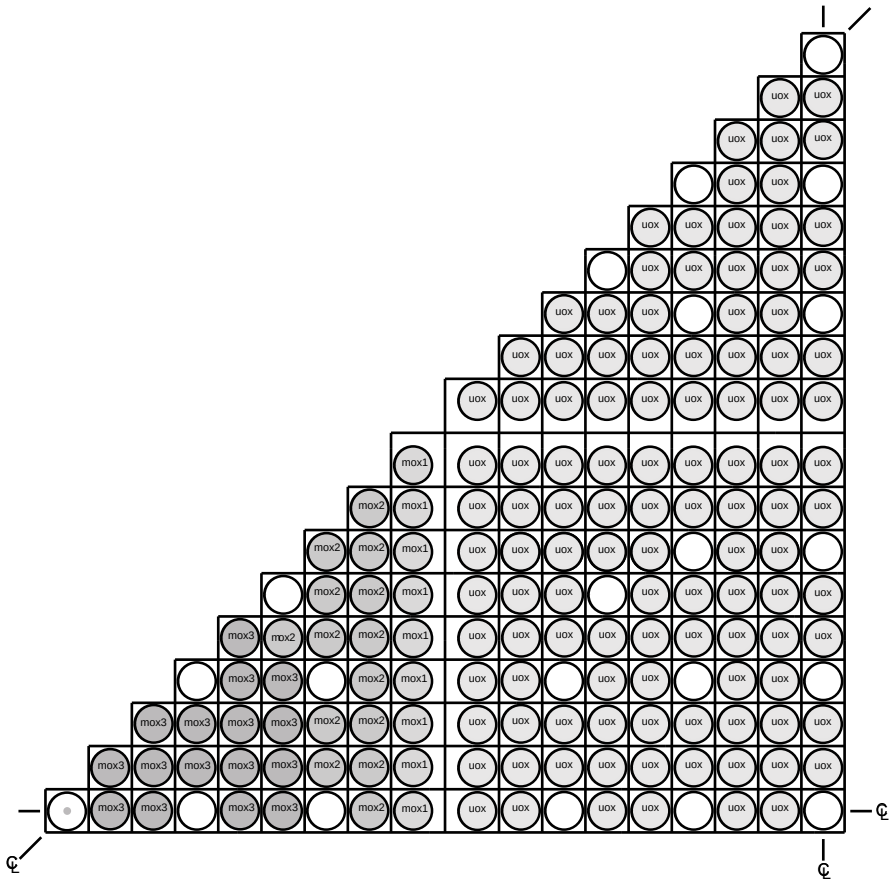

Figure 1: A MOX assembly surrounded with UOX assemblies.

Table 1: Homogenized parameters of the MOX assembly.

	diffusion coefficients (cm)		total cross sections (cm^{-1})		SPH factors (1)	
	fast group	thermal group	fast group	thermal group	fast group	thermal group
I	1.4136	0.37674	0.29735	1.1767	1.0	1.0
II	1.7913	0.28929	0.35506	0.81018	1.2048	0.68187
III	1.7290	0.25883	0.35684	0.81588	1.2111	0.68666

- The MOX lattice parameters obtained without UOX environment are far away from the results obtained with approaches **II** and **III**.
- By comparing the results of approaches **II** and **III**, we see a small streaming effect on the total cross section ($\simeq$ 0.7 %) and a larger effect on the diffusion coefficients ($\simeq$ 10.5 %).
- The correction of the SPH equivalence technique cannot be neglected.

Note that the cost overhead of the calculation **III** with respect to **II** is $\simeq$ 23 % on an Ultra SparcStation.

6 CONCLUSIONS

We have show that an isotropic streaming model can be used for thermal lattice calculations, with an acceptable cost overhead. The main benefit of this approach is to compute a space–dependant diffusion coefficient, compatible with a multi-region homogenization of the lattice. It is therefore possible to obtain assembly–dependent diffusion coefficients in a colorset calculation.

Other benefits can be expected from this approach. The availability of an heterogeneous fundamental current allows the current–weighting of the P_1 scattering cross sections and both the flux– and current–weighting of the total cross sections. This new information can be used to improve the full core calculation made with the simplified P_n method.

ACKNOWLEDGMENTS

This work was supported by EDF under contract EPAC–5C51/CANAL–3130 (Descartes project). The author is especially grateful to G. Rimpault from CEA/Cadarache for helpful discussions.

References

[Sanchez, 1987] R. Sanchez, J. Mondot, Z. Stankovsky, A. Cossic and I. Zmijarevic, "APOLLO-II: A User-Oriented, Portable, Modular Code for Multigroup Transport Assembly Calculations," *Proc. Int. Top. Mtg. Advances in Reactor Physics, Mathematics and Computation*, Paris, France, April 27–30 (1987).

[Hébert, 1993] A. Hébert, "A Consistent Technique for the Pin-by-Pin Homogenization of a Pressurized Water Reactor Assembly," *Nucl. Sci. Eng.*, **113**, 227 (1993).

[Hébert, 1997] A. Hébert, "Application of Transport Methods to Lattice Calculations", *1997 Frédéric Joliot Summer School*, Cadarache, France, p. 81, August 25 – September 3 (1997).

[Kavenoky, 1968] A. Kavenoky et M. Michel-Villaz, "Définition et calcul du coefficient de diffusion des milieux multiplicateurs à neutrons rapides, à partir d'une solution fondamentale de l'équation de Boltzmann", Commissariat à l'énergie atomique, Note SPM-710 (1968).

[Grimstone, 1990] Grimstone, M. J., Tulett, J. D. and Rimpault, G., "Accurate Treatments of Fast Reactor Fuel Assembly Heterogeneity with the ECCO Cell Code", *Proc. Int. Conf. on the Physics of Reactors: Operation, Design and Computation – PHYSOR 90*, Marseille, France, p. IX:24, April 23-27 (1990).

[Benoist, 1994] P. Benoist, J. Mondot and I. Petrovic, "Calculational and Experimental Investigations of Void Effect – A Simple Theoritical Model for Space-Dependent Leakage of Heterogeneous Assemblies", *Nucl. Sci. Eng.*, **118**, 197 (1994).

[Petrovic, 1996] I. Petrovic, P. Benoist and G. Marleau, "A Quasi-Isotropic Reflecting Boundary Condition for the TIBERE Heterogeneous Leakage Model", *Nucl. Sci. Eng.*, **122**, 151 (1996).